Letters in Applied NanoBioScience
Open-Access Journal (ISSN: 2284-6808)

Review
Volume 12, Issue 3, 2023, 68
https://doi.org/10.33263/LIANBS123.068

Carbonization of Selected Biological Materials, Trends, and Perspectives◊

Martyna Kotula [1,2,*], Anita Kubiak [1,2], Bartosz Leśniewski [1,2], Martyna Pajewska-Szmyt [2,*]

[1] Faculty of Chemistry, Adam Mickiewicz University, Uniwersytetu Poznańskiego 8, 61-614 Poznań, Poland; markot6@amu.edu.pl (M.K.); anikub@amu.edu.pl (A.K.); barles5@amu.edu.pl (B.L.);
[2] Center of Advanced Technology, Adam Mickiewicz University, Uniwersytetu Poznańskiego 10, 61-614 Poznań, Poland; mpszmyt@amu.edu.pl (M. P-Sz.);
* Correspondence: markot6@amu.edu.pl (M.K.); mpszmyt@amu.edu.pl (M. P-Sz.);
◊ Paper dedicated to Professor Hermann Ehrlich on the Occasion of His 65th Birthday.

Scopus Author ID 57205603979
Received: 14.02.2022; Accepted: 17.03.2022; Published: 18.04.2022

Abstract: The exploration of new materials as well as methods and sources of their production is a constantly growing trend in both scientific and industrial directions. One such method is carbonization, which has attracted a lot of attention over the past decades. Carbonization is the process of preparation of 3D carbonaceous materials with unique properties by thermal treatments with the exclusion of oxygen. A higher specific surface area characterizes the obtained nanoporous carbon materials compared to their precursors, and, consequently, they can be used in such fields as biotechnology, electrochemistry, or electronic industry. Special attention has been directed to the carbonization of nanoorganized biological materials due to their extensive composition and unique hierarchical structure. This review aims to provide insight into the examples of carbonization of selected biomaterials such as polysaccharides (cellulose, chitin) and proteins (keratin, spongin, silk) evidenced by excellent and successful examples from the recent literature. In addition, this work highlights the most significant aspects of diverse experiments, allowing getting inspiration for fields such as materials science and well extreme biomimetics.

Keywords: carbonization; biological materials; cellulose; chitin; keratin; spongin; silk

1. Introduction

Carbonization is a process referring to the transformation of three-dimensional (3D) organic macromolecules into a 3D "macro-atomic" network of carbon atoms during gradual heating. Small molecules (carbon dioxide, methanol, water) are removed from the organic system during the carbonization process. This process does not produce a continuous solid phase but a phase with nanometer-sized spaces - a porous 3D carbon network [1]. There are several processes for converting the starting material into a carbon-rich solid. Depending on the subsequent application, carbon can be obtained by pyrolysis, torrefaction, or hydrothermal carbonization. The main difference is the medium used. In the case of hydrothermal processes, the processes take place in water under subcritical or supercritical conditions, used especially for moist raw materials. Pyrolysis is a transformation under high temperatures without oxygen [2].

Biological materials (silk, keratin, collagen, spongin, chitin, cellulose, bone, dentin etc.) are materials produced solely by biological systems (Figure 1) [3]. They are more complex

materials than synthetic materials due to their hierarchical structure and multifunctionality [4,5]. Biological materials can be classified into soft and hard due to their mechanical properties. Soft biological materials build muscles, skin and internal organs, etc. Hard materials constitute the skeleton from which nails and teeth are built in vertebrates and the exoskeleton in arthropods [6].

Despite their well-recognized applications in biomedicine and tissue engineering, biological materials remain the focus of extreme biomimetics [7] and bioinspired materials science [8,9]. Extreme biomimetics is an attractive research direction that uses elements and models of nature to develop a new generation of biologically inspired and functional nanostructured composite materials [10]. The essential concept of this approach is to use biopolymers that are characterized by chemical and thermal resistance under these very particular *in vitro* conditions. Such research can lead to a greater understanding of the origin of life in harsh environments and new methods for creating novel composite materials with utterly new physicochemical properties [7]. Carbonization of appropriative structural biological materials is one of the directions within extreme biomimetics [11].

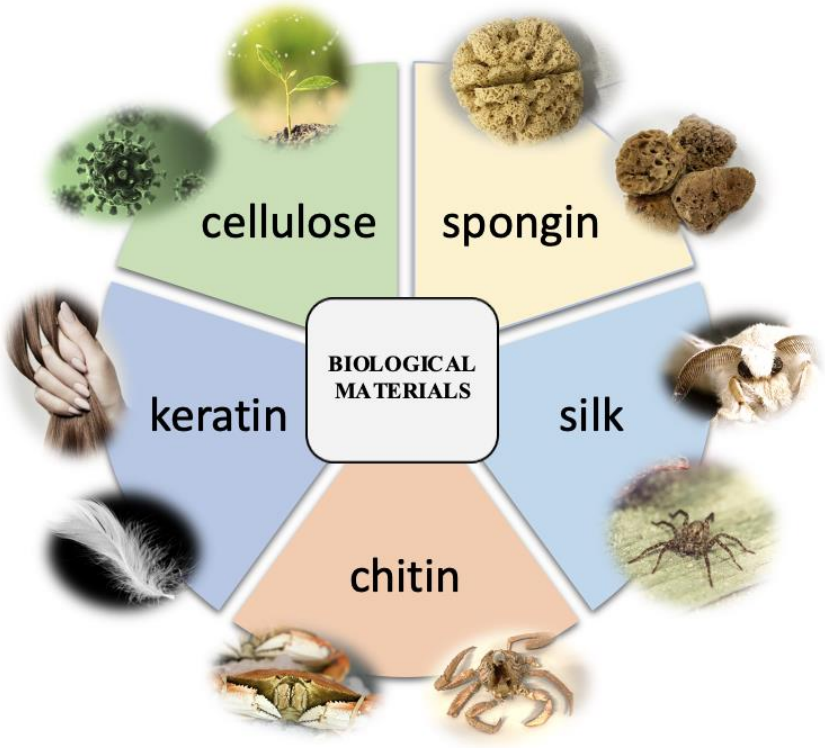

Figure 1. Selected biological materials and their source.

In recent years, more attention has been paid to porous carbon materials due to their remarkable performance in various applications. The structure and parameters of the blanket carbonaceous material depend on the carbon source. The number of literature reports on carbonaceous materials derived from biological materials is steadily increasing. Most of the biopolymers such as silk [12,13], cellulose [14,15], chitin [16,17], keratin [18,19], spongin [11,20], etc.) can be successfully used as precursors of corresponding carbon materials. Producing carbon materials with controlled microstructure and morphology, especially at large scales and from renewable and biodegradable natural sources, is a current trend in materials science [21].

In today's modern world seeking high environmental applications, biological materials have gained significant interest. Sustainable natural resources are utilized because of their

potential to produce a variety of high-value products with low environmental impact. Composites containing biological materials with nanostructured architecture provide both interesting chemical properties and inspiration for biomimetic research [22]. The interest in the carbonization process, especially for biomass [23,24], stems from the fact that they open the possibility of creating new carbon materials with improved physicochemical properties, novel nanostructures, and the presence of heteroatoms, or hierarchical porosity. Knowledge of the elementary mechanisms and reactions can help gain these characteristics by adjusting process conditions. As reviewed below, such functionalized carbons are used in various fields.

2. Carbonization of Structured Polysaccharides

2.1. Cellulose.

Cellulose is one of the most abundant biopolymers on earth [25]. The total cellulose production is about 10^{11}-10^{12} tons per year [26,27]. Thus, it presents an enormous amount of renewable and biodegradable resources for raw materials. In addition to plants, which are the main source of cellulose, selected bacteria such as *Gluconacetobacter, Aerobacter, Azobacter Achromobacter, Salmonella, Pseudomonas, Rhizobium, Alcaligenes* as well as oomycetes and algae are also able to produce cellulose [28–30]. Regardless of its source, each cellulose chain is made up of anhydro-D-glucose molecules linked by β-1-glycosidic bonds [31]. Bacterial cellulose (BC) was first accidentally discovered during vinegar fermentation in 1886 by Brown [32]. Since then, numerous studies conducted in this field have confirmed its unique properties. BC and its derivatives have been shown to have great potential in various applications such as biomedicine [33], and electronics [34] (for a recent overview, see [35]).

For the first time, Zhu and co-workers [36] converted pure cellulose nanocrystals (CNCs) extracted from wood into porous carbon with a defined network structure and per located carbon nanofibers by carbonization at relatively low temperature (1000°C) (Figure 2), and then used them as anode for sodium-ion batteries (SIBs). The electrochemical properties of the CNC-derived carbon showed promise. The obtained porous carbon exhibited excellent properties, including a high reversible capacity of 340 mAh/g at a current density of 100 mA/g, one of the highest capacities of carbon anodes for SIBs.

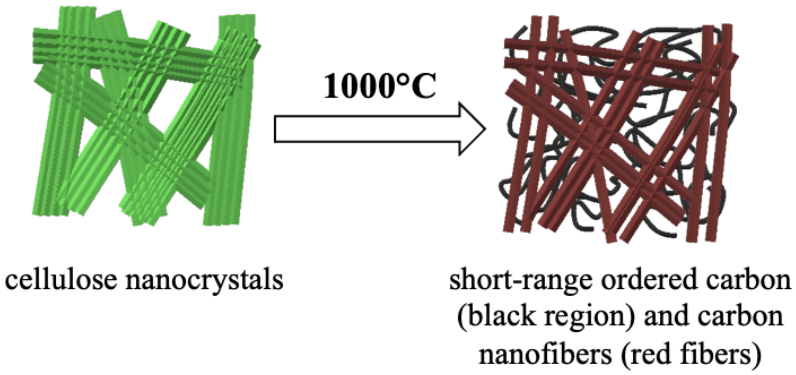

Figure 2. Scheme showing the transformation of cellulose nanocrystals into percolated conductive carbon by carbonization.

In 2018, Feng and co-workers [37] obtained carbon nanospheres (CNs) from cellulose by microwave-assisted hydrothermal carbonization. The carbon materials were adsorbents for trace amounts of pharmaceuticals such as diclofenac sodium (DCF) in aqueous solutions. The removal efficiencies of diclofenac by CN were 100 % removal of 0.001 mg/mL DCF within

30 seconds and 59 % removal of 0.01 mg/mL DCF within 1 hour, respectively. In addition, the effective adsorption capacity was also observed against three other commonly detected contaminants in wastewater - diphenylamine (DPA), benzophenone (BZP), and ketoprofen (KP). The methodology presented in this study provides further insight into drug adsorption on cellulosic carbon adsorbents and the application of biodegradable carbons in the treatment of pharmaceutical-contaminated wastewater [37].

Hydrochar microspheres have great potential for use in biomass valorization to produce value-added compounds. They represent easy to process and clean carbon materials. Sheng's group investigated the feasibility of using hydrochars from cellulose and xylan for biofuel production in 2019 [38]. The obtained results showed that the specific surface area (S_{BET}) of cellulose-derived hydrochar is higher than xylan-derived hydrochar (118 m^2/g >28 m^2/g). Hence, Al catalyst (Al-Cel-HTC) for glucose isomerization was obtained by the one-step hydrothermal process of cellulose-derived hydrochar. The catalytic performance results of Al-Cel-HTC indicate that 13.4% fructose can be obtained from glucose isomerization with high selectivity (77.8 mol/%) [38].

Despite the great progress in obtaining carbon nanospheres, their utilization in LIB cells is still a great challenge. In recent years, with the rapid development of energy technologies, more attention has been paid to the synthesis of carbon materials for the anode of lithium-ion batteries (LIBs) with biomass as a resource. Carbon materials such as carbon nanospheres (CCS) based on cellulose were synthesized by Yu and co-workers [39] by performing hydrothermal carbonization (HTC). They used corn straw, which is a waste material from agricultural fields, as raw material. They used the obtained carbonaceous material as an electrode for LIB. By carefully controlling the reaction time, they captured the most optimal conditions. The carbon products obtained after carbonization for 36 h showed excellent chemical stability and specific capacitance of 577 mA h g^{-1} after 100 cycles at 0.2C. This work presents an environmentally friendly and efficient method to produce CCS from corn straw and opens new opportunities for anode LIBs [39].

In 2020, Adolffson and co-workers [40] in their study described cationized cellulose filters with an oxidized carbonized cellulose (OCC) coating. The cellulose filters were treated with the following reagents as 3-chloro-2-hydroxypropyltrimethylammonium chloride (CHTAC) and sodium hydroxide. OCC was obtained by hydrothermal carbonization of biopolymer - cellulose and further steps such as oxidation and dialysis. After that, they were connected to the cationized filters by electrostatic interactions. The application of filters based on adsorbed the mode of pollution methylene blue (MB) from an aqueous solution and MB could then be found on the filter surfaces by surface-assisted desorption ionization-mass spectrometry (SALDI-MS). This innovative study provides the promising potential of OCC-coated filters as combination surfaces for use in the quick monitoring of environmental impurities [40].

Recently, also cellulose-based composites have been used for the development of carbon fibers. Bengtsson and co-workers [41] prepared carbon fibers (CF) from a lignin-cellulose precursor (a mixture of softwood kraft lignin (SKL) and bleached softwood sulfate pulp (KP)) by a fixation process and determined what effect carbonization time and temperature have on CF properties. It was shown that reducing the time does not significantly affect the tensile properties and that the temperature range of 600-800°C is the critical point of carbonization where there is a significant increase in tensile properties (from 360 to 810 MPa). The highest Young's modulus (77 GPa) was secured during the carbonization process at

1600°C, which suggests a gradual transformation of CF from amorphous to nanocrystalline graphite, while the material obtained at 1000°C has the highest tensile strength (1050 MPa), which may be due to the increase in radial heterogeneity [41].

So far, the mechanism of structural transformation and how the different biomass components interact with each other during thermal decomposition are not fully elucidated. In 2021, Meng and co-workers [42] in their study focused attention on the structure evolution of nanocellulose and lignin during carbonization. The carbonization of both precursors under the same conditions in the temperature range of 320 to 950°C resulted in two types of carbons. It was observed that cellulose forms a nanoporous structure typical of porous carbons, while lignin-derived carbon forms graphite sheet and onion structures that indicate partial graphitization. The presented studies can provide a basis for understanding the carbonization mechanism of key biomass components and encourage further research on modifying their structure to obtain better properties [42].

2.2. Chitin.

Chitin is the second most widely encountered natural carbohydrate polymer after cellulose [43]. Its total production is approximately 10^{10}-10^{11} tons annually [44]. Chitin comprises of β-(1,4)-linked-2-acetamido-2-deoxy-d-glucopyranose units with significant amidogen and hydroxyl groups [45]; hence it has great potential in obtaining N-enriched carbons for supercapacitors [46,47]. Moreover, it attracts special interest due to its high availability, non-toxicity, and biodegradability. Chitin occurs in nature as ordered crystalline microfibrils forming structural components in the cell walls of diatoms [48], yeast, and fungi, as well in the exoskeletons of selected corals [49,50], sponges [51–55], as well as diverse arthropods [56,57]. It is also produced by many other living organisms in the lower plant and animal kingdoms, performing many functions where strength and durability are required [58–60]. Despite the widespread occurrence of chitin, the main commercial sources of chitin have been crabs and shrimp shells [61]. Only recently, naturally prestructured and ready-to-use chitin scaffolds of poriferan origin remain to be in the focus of tissue engineering [62–64] and material science [65–68].

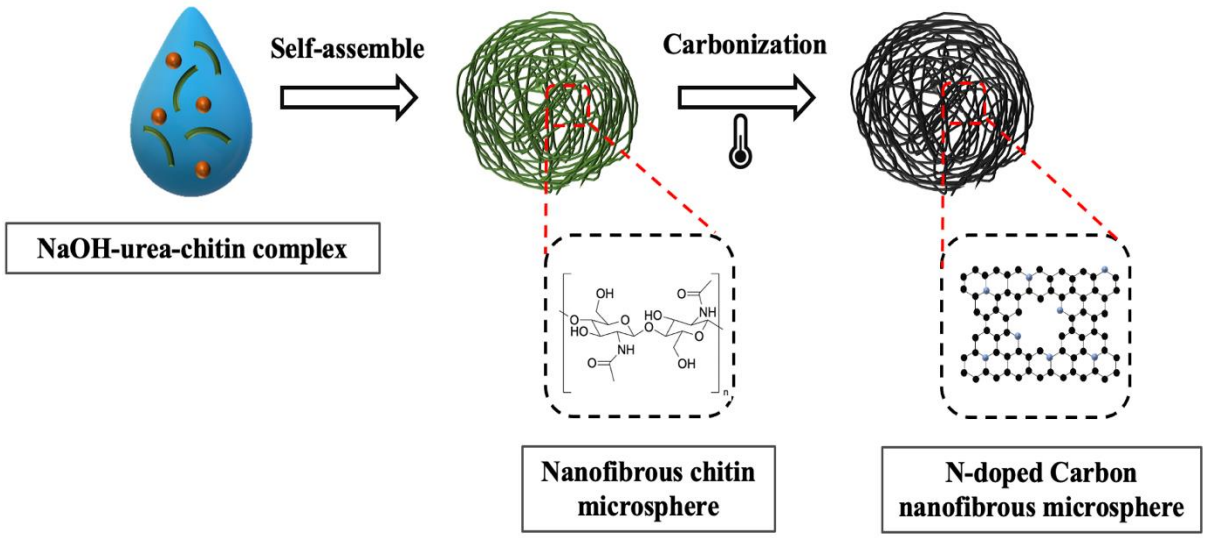

Figure 3. Scheme for obtaining nanofibrous carbon microspheres.

Conversion of small value biomass wastes (carbonization, etc.) into valuable and useful materials can benefit the environment and create high value-added chitin. Especially the fact

that many biomass materials, including chitin, are naturally rich in heteroatoms (oxygen, nitrogen), and after pyrolysis at high temperature and in an inert atmosphere, it is possible to convert into stable heteroatom admix carbon materials. Duan and co-workers [69] prepared N-doped nanofibrous microspheres by dissolving chitin in an aqueous NaOH/urea solvent followed by carbonization (Figure 3). The prepared carbon material exhibited a high specific surface area (more than 1000 m^2/g) and stable 3D-connected lattice structure and was successfully applied in supercapacitors.

Wang and co-workers [70] developed a novel method to receive hierarchical porous material based on carbon modified with heteroatoms obtained from chitin using $KMnO_4$ reagent as a crucial activator and stencil precursor with hydroxyl and amidogen. Optimization of the synthesis yielded hierarchical porous carbon materials (HPC-700) characterized by large specific surface area and numerous oxygen and nitrogen functional groups, resulting in an HPC-700 electrode with very high specific capacitance (412.5 F g^{-1} at 0.5 A g^{-1}) and satisfactory electrochemical stability (only 0.4% loss after 10,000 cycles). Moreover, the developed flexible material as an all-solid-state supercapacitor exhibited high energy density (9.67 Wh Kg^{-1}) and excellent electrochemical stability in PVA/KOH electrolyte sol. This synthesis approach can promote the use of biomass as a carbon source and applications in the field of energy storage systems.

Another approach was presented by Zheng and co-workers [71], who fabricated nitrogen-doped carbon nanospheres with ordered microporous structure by direct pyrolysis of chitin nanogels. The obtained nanospheres had a 20-30 nm diameter and a high specific surface area of 1363 m^2/g. Besides, the porous carbon nanospheres preserved a nitrogen element content of 3.2% and desirable conductivity properties. Furthermore, the capacitor electrodes prepared from carbon nanospheres obtained by pyrolysis at 800°C (CNC-800) exhibited a capacitance of 192 F g–1 at a current density of 0.5 A exceptional cycling stability.

In 2021, Jiang and co-workers [72] successfully synthesized heteroatom-doped porous carbon (CL) by pyrolysis without using an activation reagent. They used biomass waste chitin with lignosulfonate as a precursor, which was a natural sulfur doping agent. The obtained CLs used as electrode materials exhibited excellent electrochemical properties - high reversible specific capacitance (644.5 mA h g at a current density of 50 mA g^{-1}) and stable cycling resistance (after 300 cycles at a current density of 100 mA g^{-1}, a specific capacitance of 350.7 mA g^{-1} was still maintained).

Zero-dimensional carbon materials, including quantum dots of biological origin, have started to play an increasingly important role in bioimaging, biosensor applications, and photocatalysis. This is due to their ease of preparation and functionalization, low cost, and their characteristics - excellent physicochemical and photochemical stability and low toxicity [73,74]. Up to now, there have been few reports on the preparation of quantum dots from chitin as a precursor. In these reports, chitin usually required pretreatment to remove the acetyl group or to form chitin nanofibers [75,76]. In 2020, Jiang's group [77] reported a procedure to prepare nitrogen-doped quantum dots (N-CQDs) from chitin as a precursor but without pretreatment and the addition of ammonia as a passivator. Ammonia accelerated the degradation and hydrothermal carbonization of chitin and provided an additional nitrogen source. The obtained N-CDQs with spheroidal morphology (diameter 4.21 nm) exhibited photoluminescence under UV irradiation and provided a good fluorescent sensor for ClO^- detection.

Elimination of contaminants in the water is possible, among other things, through adsorption technology. Activated carbon is the most used adsorbent due to its unique intrinsic

properties. Ji and co-workers [78] prepared carbon materials by carbonization followed by chemical activation (KOH) of chitinous biomass. The resulting highly porous activated carbon had a high BET specific surface area (2186.3 m^2/g) and total pore volume (0.9815 cm^3/g). It was also found to be a good adsorbent for the removal of cationic Crystal Violet (CV) dye from solution for a large pH range, with removal efficiencies close to 100%. Khanday and co-workers [79] characterized activated carbons (ACs) with relatively large BET surface area (1199.02 m^2/g) produced by single-step chitin pyrolysis and phosphoric acid activation. The generated carbons were used in the adsorption of the antibiotic cephalexin (CFX). Compared with the activated carbons from other precursors, the activated carbons from chitin had higher adsorption capacity toward CFX; the maximum monolayer adsorption capacity reached 245.19 mg/g at 50°C. Hence, this work confirms that ACs from chitin represent an effective and economical adsorbent both for particles and antibiotics and for removing various contaminants from water.

3. Carbonization of Structural Proteins

3.1. Keratin.

Keratin is an example of a structural protein that associates with intermediate filaments of vertebrates forming the bulk of cytoskeleton and epidermal appendageal structures such as nails, hair, feathers, horns, and wool [80]. Also, marine fish (sharks; hagfish), birds, mammals (whales, dolphins, porpoises), and reptilians (turtles, crocodilian) contain keratins in the form of intermediate filaments (IFs). These filaments are primarily strictly intracellular entities except marine fish, which secrete intermediate filaments in defensive mucus [4,81].

Keratin is rich in such elements as oxygen, hydrogen, nitrogen, sulfur, and trace amounts of Mg, Fe, among others [82]. There are hard keratins with higher amounts of sulfur, which mainly build the structure of the hard epidermis, and soft keratins with lower amounts that provide elasticity to epithelial tissues (epidermis) [83]. Keratin wastes such as those from the butchery industry (e.g., animal hairs, feathers, and horns) and from textiles (wool materials) are annually generated at 8.6 million tons and 2.5 million tons, respectively [84,85]. Therefore, it remains in nature, causing various types of contamination. The best way to solve these problems is to use bio-waste as a resource.

Recently, keratin-based materials have attracted more attention due to their ability to be converted into more useful forms. A variety of keratin-based biomaterials such as films, fibers, hydrogels, and sponges have made them applicable in the field of biomedical sciences. Due to the fact that these biomaterials are biocompatible, durable, biodegradable, and have the ability of cell proliferation, which makes them excellent candidates in tissue engineering and drug delivery systems [86,87] (for a recent overview, see also [88]).

Human hair is also a common bio-waste that is mainly composed of heteroatom-containing amino acids [89]. It represents one of the most abundant keratin wastes, which slowly decomposes over time by releasing its constituent elements carbon, sulfur, nitrogen, and oxygen into nature [90]. Therefore, it remains in nature, causing various types of contamination. The best way to solve these problems is to use bio-waste as a resource. Activated carbons obtained from human hair are being investigated for diverse applications modes, for instance, electrochemical sensors [91], gas absorption [92,93], electrocatalysis [94], electrode materials for solar cells [95], and supercapacitors [18,96–98] (Figure 4).

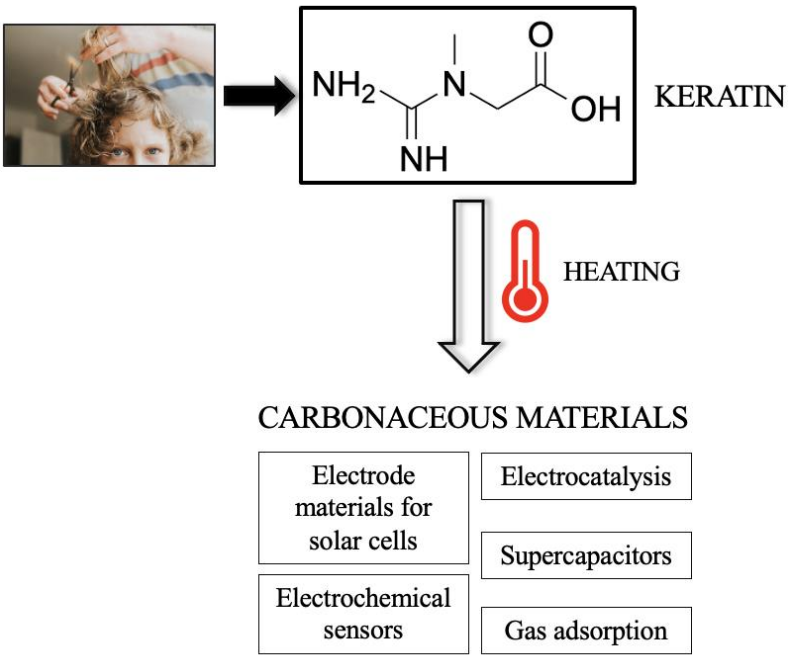

Figure 4. Applications of keratin-derived carbon materials [18,91–98].

Martin Parrondo and Bagriantsev [99] have patented a method to synthesize synthetic diamond monocrystals of different colors from carbon obtained by carbonizing keratin contained in human or animal hair and then subjecting it to a high-temperature and high-pressure process.

Pramanick and co-workers [91] prepared carbon microfibers by pyrolysis of human hair and applied them successfully for electrochemical detection of ascorbic acid and dopamine. Ahmed and co-workers [92] synthesized porous carbon material (HHC) by KOH activation for the adsorption of tetracycline antibiotics (TC). HHC showed a high surface area of 1505.11 m^2/g and 68.34% microporosity; the maximum monolayer adsorption capacity for TC was 128.52 mg/g at 30°C. Zhao and co-workers [93] successfully synthesized nitrogen- and sulfur-doped porous carbon materials from human hair *via* a simple method based on the following steps degradation and, finally, carbonization/chemical activation phase. The received novel carbon materials had large specific surface areas (up to 2700 m^2/g) and excellent gas sorption properties: carbon dioxide uptake (up to 24.0 wt%, at 273 K and 1.0 bar), methane adsorption (up to 3.04 wt%, at 273 K and 1.0 bar), and hydrogen adsorption (up to 2.03 wt%, at 77 K and 1.0 bar). Freitas and co-workers [94] developed a highly efficient and active electrocatalyst for hydrogen evolution reaction (HER). Porous carbon doped with N and S obtained by pyrolysis of human hair showed high activity for hydrogen evolution with a low overpotential of only -12 mV, a Tafel slope of 57.4 mV dec^{-1}, a current density of 10 mA cm^{-2} at - 0.1 V vs. RHE, and remarkable durability. This performance was highly similar to that of commercial 20 wt% Pt/C catalysts. Sahasrabudhe *et al*. [95] received highly electrocatalytic porous graphitic carbon (GPC) by simple carbonization from bio-waste of human hair without an activation process. The carbon obtained in this way was first used in quantum dot sensitized solar cells (QDSC) in the form of catalytic counter electrodes (CE). The spectacular PCE of 4.44% achieved during optimization GPC CE was found to overtake that of other contemporary CE materials such as Pt and active commercial carbon; however, similar to the widely used material as CuxS CEs. Si and co-workers [96] synthesized nitrogen- and sulfur-doped carbon material by hydrothermal carbonization of human hair and glucose as carbon precursors followed by KOH

activation. They applied the resulting carbon in a supercapacitor, obtaining a specific capacitance of 264 F g^{-1} with a very low current density of 0.25 A g^{-1}, which dropped to 154 F g^{-1} after only 1000 cycles. Quian and co-workers [18] obtained heteroatom-doped activated carbon flakes for a supercapacitor electrode *via* carbonization of human hair fibers followed by activation with KOH. The capacitance value for the carbon was 340 F g^{-1} at a current density of 1A g^{-1} and good stability over 20,000 cycles. However, a toxic organic electrolyte was used to produce the supercapacitor, which has adverse environmental effects. In 2020, Siha and co-workers [98] obtained activated carbon sheets, which they used as ultra-high quality electrode material in supercapacitors. Human hair was carbonized at 900°C and activated with KOH, resulting in nanometer-thick carbon sheets with a specific surface area of 1548 m^2/g. The electrode material prepared from this carbon shows an exceptional specific capacitance of 999 F g^{-1} at a current density of 1 A g^{-1}. Also, the symmetrical supercapacitor assembled from it provides an excellent energy density of 32 W h Kg^{-1} at a power density of 325 W Kg^{-1} and retains up to 21.4 W h Kg^{-1} even at a very high-power density of 8125 W Kg^{-1}. Besides, it shows high cyclic stability, retaining 98% of the initial capacitance value after 10,000 continuous GCD cycles at a high current density of 5 A g^{-1} using 6 M KOH as the electrolyte [98].

Human fingernails, which can be easily extracted from nail salon waste, are also a promising precursor for synthesizing carbon materials. Chatzimitakos and co-workers [100] reported an efficient method to synthesize multifunctional carbon nanodots (CDNs) by carbonization at 200°C of human fingernails. The obtained CDNs were used to prepare an ultra-sensitive probe for Cr(VI) detection based on a combination of internal filter and static quenching mechanism. The performed studies showed that the CDNs promote cell proliferation, are compatible with blood, and are suitable for cell imaging, making them suitable for more advanced biological applications.

Chicken feathers are composed of keratin tubes with an α-helix structure filled with keratin with a β-helix structure [101]. After their carbonization and activation, it is possible to obtain a homogeneous porous material with a large BET surface area. Due to economic and environmental reasons, chicken feathers are increasingly used as carbon precursors for applications, including as electrode materials for supercapacitors [102,103], electrocatalysts [104], and adsorbents [105–108]. Hastuti and co-workers [109] prepared activated carbon from chicken feathers and investigated its use as an electrode material for lithium-ion batteries. The carbon materials were obtained by pyrolysis at 700°C, which were then activated using different concentrations of KOH. The optimized material used as electrode material showed a high discharge capacity of 445.87 $mAhg^{-1}$ and maintained a Coulombic efficiency of almost 100%. In 2020, Rangaraj and co-workers [110] developed a zinc sulfide composite doped with carbon material obtained by carbonization of chicken feathers (ZnSCFC). The obtained composite used as anode material for Li-ion batteries shows a reversible capacity of 788 mAh g^{-1} after 150 cycles at 100 mA g^{-1}.

A commonly used method for fiber production is electrospinning. With this method, well-defined fibers with nanometer diameters can be obtained using different types of polymeric diluents. Villanueva and co-workers [111], in their study for the electrospinning process, used polyacrylonitrile (PAN) dissolved in N,N-dimethylformamide (DMF) with the addition of keratin solution (5%, 7%, 10% solution volume) from chicken feathers to improve the electrical properties of fibers. The study indicates that electrospun carbon nanofibers based on PAN and keratin can be potential electrodes for asymmetric supercapacitors.

3.2. Spongin.

Spongin is the fibrous skeletal proteinaceous composite [112] of sponges belonging to the class Demospongiae (phylum Porifera), which are cultivated worldwide and are a renewable biological material that can be produced on a large scale [113]. According to Ehrlich [5], spongin is not a pure protein structure but rather a type of collagen-based composite that combines with halogenated and Ca- and Si-containing fibrillar structures, resulting in a dense network of nanofibrils [114]. The sponginous structure is formed by single fibers up to 100 nm thick and composed of nanofibers that interconnect into complex hierarchical 3D networks with high porosity (Figure 5). This structure of spongin is responsible for its unique physicochemical and mechanical properties [115,116] and provides high thermal stability up to 360°C [117]. Therefore, marine bath sponges are an efficient model for developing new 3D composites with hierarchical structures using biodegradable and non-toxic organic scaffolds [20,65].

During 600 million years of evolution, marine demosponges produced structures ranging from centimeters to meters [116]. Since ancient times, spongin-based 3D skeletons have been known as bath sponges or commercial sponges. The intensive farming of marine sponges worldwide and market volume of $20 million per year was largely limited to cosmetic and simple medical applications only [116]. Although the structural variety of marine sponge skeletons as a biological material is still not completely uncovered, numerous literature studies emerging recently on sponge-based skeleton materials prove that it is a renewable source of naturally occurring prestructured 3D constructs with convenient, practical application in various fields like biomedicine, tissue engineering as well technology [5,67,118–121]

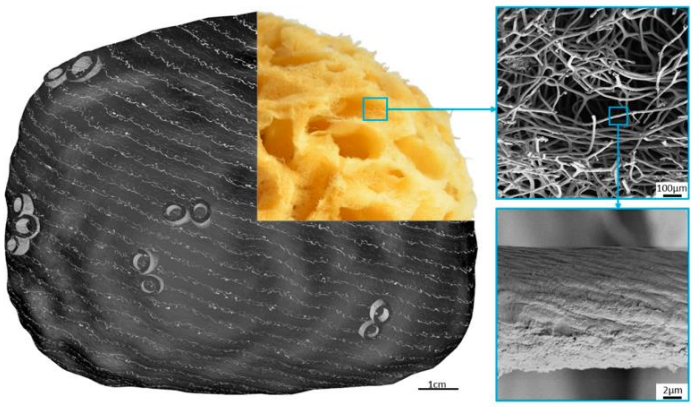

Figure 5. Schematic view of the structure of sponges. The SEM images on the right show the sponge-based skeleton structure. Reprinted from [116] (licensed under CC BY 4.0).

Due to spongin's acid resistance and thermostability (up to 350°C), several successful attempts to use this biopolymer as a scaffold in extreme biomimetic approaches have been reported since 2015. Szatkowski and co-workers [122] used this biological material for the hydrothermal treatment of hematite (α-Fe_2O_3) at 90°C using a reagent as $FeCl_3$ to get a hematite-sponge-like scaffold. The resulting material Fe_2O_3/spongin was tested for use as an anode material in a capacitor. The outcomes show that components built on this novel composite (α-Fe_2O_3-spongin) have a beneficial impact on the capacitance of energy carriers. The same research group [123] also produced another composite by immobilizing TiO_2 on 3D spongin scaffolds at 120°C. The use of the obtained composite as a photocatalyst for the removal of dyes (Methylene Blue [122], C.I. Basic Blue [10]) showed promising results for

both sorption and photocatalytic processes. In another paper, Akbari and co-workers [120] described a magnetic composite based on a 3D spongin scaffold with nanoscale Fe_3O_4 cores for organic wastewater treatment applications. The obtained composite efficiently adsorbed cationic dyes such as methylene blue (MB) and crystal violet (CV). Besides, the good adsorption properties of this material make it a potential drug carrier. For the past few years, a new trend in extreme biomimetics has been the design of spongin-based 3D scaffolds at 500°C in an oxygen-free atmosphere.

Szatkowski and co-workers [20] described the synthesis of a novel nanostructured MnO_2-based 3D composite by an extreme biomimetics approach. The MnO_2/carbonized spongin composite is characterized by a unique spongin carbon fiber network (carbonized at 650°C) and a defined nanoscale manganese oxide structure. The resulting composite exhibits a bimodal pore distribution, with macropores derived from the sponge network and mesopores from the nanostructured oxide coating. Moreover, the composite exhibited better electrochemical properties when equated to MnO_2, and voltammetry cycling showed it to be stable over 300 charge/discharge cycles. In 2019, Petrenko and co-workers [11] presented the first successful design of a centimeter-scale 3D spongin-Cu/Cu_2O material using an extreme biomimetic strategy. The thermostability of this collagenous raw material at temperatures up to 1200°C enables the fabrication of 3D fibrous and nanoporous turbostatic graphite up to 4 x 10 cm large (Figure 6).

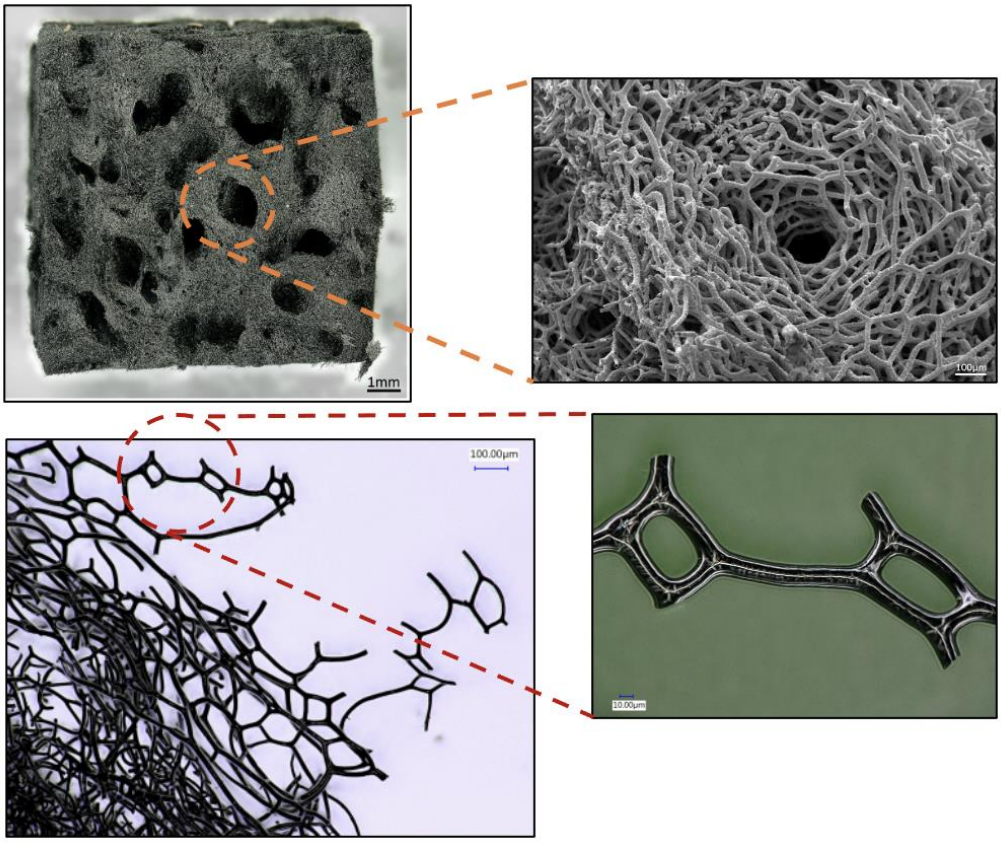

Figure 6. Turbostratic graphite-based 3D scaffold obtained after carbonization of microfibrous spongin at 1200°C.

Furthermore, the obtained results confirm that the turbostatic graphite is unique in retaining the nanostructural features typical for triple-helix collagen. The copper electroplating of the material performed yielded a hybrid material that could successfully catalyze the reduction of 4-nitrophenol (4-NP) to 4-aminophenol (4-AP) in both marine and freshwater

environments. In another paper, Żółtowska and co-workers [124] described the synthesis of three different cobalt oxide-based catalysts that were obtained by carbonization of spongin skeletons (400, 500, 600°C) and their functionalization by a simple sorption-reduction method. The tests performed confirmed the presence of a metal-containing phase (mainly Co_3O_4) that covered the carbonized spongin fibers. The carbon-based composite obtained at 600°C showed comparable to other materials reported in the literature ability to oxidize styrene, decolorize rhodamine B, and reduce 4-nitrophenol. Besides, all the obtained materials showed profitable activity in reducing 4-nitrophenol and can be reused even after the fifth catalytic cycle. The same group [125] reported a method to synthesize novel 3D fibrous-like $NiO/Ni(OH)_2$/Ni-carbonized spongin-based materials and investigated their potential use as catalysts in model reactions. Low-temperature carbonization (400, 500, 600°C) of sponge-based scaffolds yielded hierarchical 3D carbon structures with the original sponge skeleton morphology, which were then modified with nickel compound (nickel nitrate). The obtained new catalysts were subjected to catalytic studies, which showed high efficiency in reducing 4-nitrophenol and oxidation of phenolic compounds in water. Depending on the substrate used, the oxidation yields were up to 99% for 4-chlorophenoxyacetic acid (4-CPA) and methylchlorophenoxypropionic acid (MCPP) and from 80% for phenol at pH2.

3.3. Silk.

Silk belongs to the class of structural fibrous proteins to be found mostly in arthropods, mainly silkworms (*Bombyx mori, Atheraea pernyi*) and spiders (*Nephila clavipes and Araneus diadematus*) (Figure 7a) [126] as well as in marine amphipods [127]. Silk proteins are usually produced in specialized glands, then spun into fibers [128].

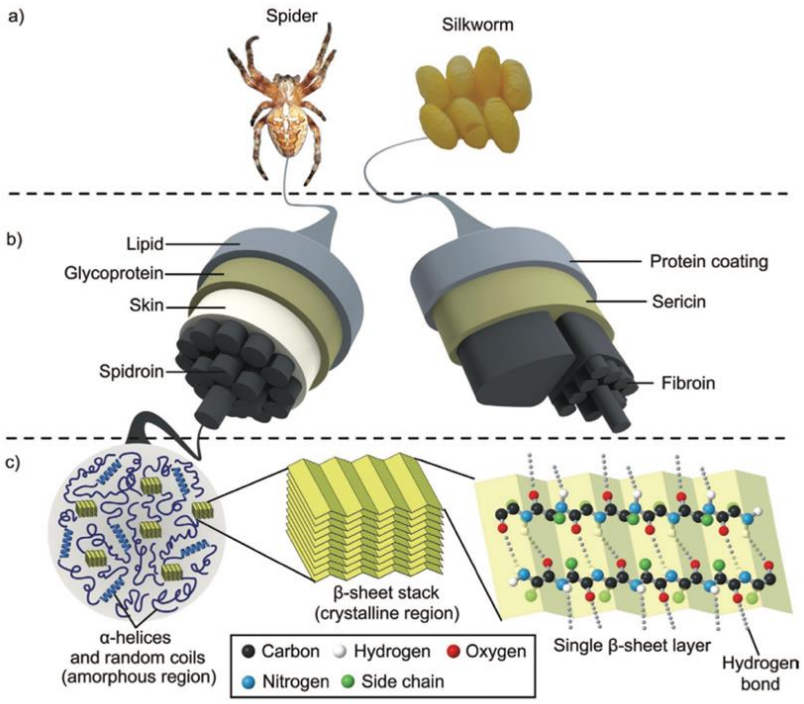

Figure 7. (a) Natural sources of silk; (**b)** The different hierarchical structures of fibers from the spider *Araneus diadematus* and the silkworm *B. mori;* (**c)** Schematics of the secondary structures of silk. Adapted from [134] (licensed under CC BY-NC 4.0, modification of section a) from original).

The silks of various arthropods show differences on a macroscopic scale (e.g., in the hierarchical organization [129,130]). Silkworm fibroin fibrils are packed into two parallel cores

that are sheathed in sericin, whereas spider fibroin fibers are packed into a single core sheathed by layers of lipids and glycoproteins (Figure 7b). At the molecular level, silk fibroins of different species consist of long chains of amino acids whose branches interact with each other to form 2D structures such as helices, α-helices, and β-sheets (Figure 7c) [130]. The most stable 2D structures are β-sheets, which are formed by numerous hydrogen bonds organized between polypeptide chains. This structure is associated with corresponding functions in protein materials, for example, the unique mechanical properties of spider silk or worm silk [131,132] and their misaggregation leading to Alzheimer's and Parkinson's diseases [133]. Silk proteins have attracted a lot of attention from scientists, especially because they do not undergo combustion at elevated temperatures but are converted into pyroprotein (carbonaceous solid). A more detailed study on the carbonization mechanism of silk proteins was carried out by Cho and co-workers [12], who found that β-sheets are converted into hexagonal carbon structures upon heating up to 350°C, while graphitic structures are formed upon heating up to 2800°C.

Silk fibroin (SF) extracted from the silkworm bombyx mori is characterized by a rich amino-group structure - β-sheets and β-crystalline structures are present [135]. This structure determines that the obtained biomass has excellent mechanical properties [132], is biocompatible, and is easy to be chemically modified, making silk a promising material for biological applications [136]. Additionally, by simple heat treatment, SF can be converted into highly catalytic carbonized silk fibroin (CSF) materials rich in N-finding applications as electrocatalysts [135], sensors [137], and flexible electronics [136].

One of the fibrous materials found in nature is spider webs (Figure 8) available on a micro-scale. Due to their good properties, including durability, flexibility, and degradability, they are good materials for obtaining carbon fibers. There are many reports in the literature on the study of obtaining carbon materials from spider webs [12,138,139].

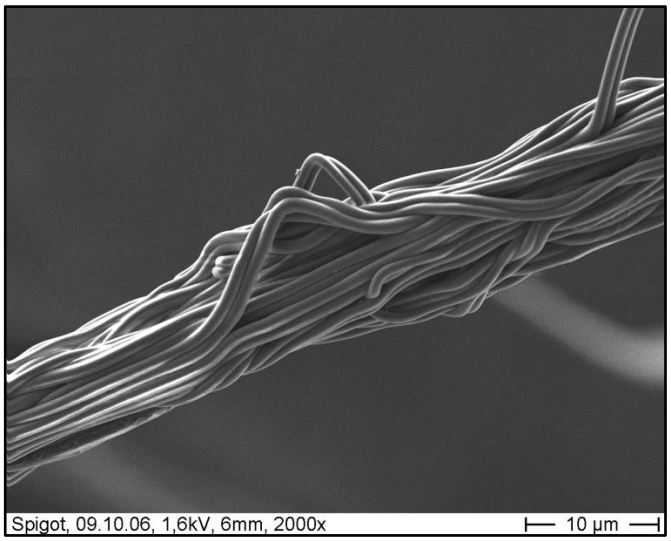

Figure 8. SEM image of spider's web.

One type of silk functionalization to improve mechanical properties, durability, etc., is an efficient and low-cost strategy to combine spinning with the continuous dip-coating technique to produce thermochromic silks (TCS). In 2021, Wang and co-workers [140] developed TCS with extremely long length (>10 km) and exceptional strength and toughness. Thermochromic silks woven into arbitrary fabrics could potentially be used in wearable devices, smart textiles, or flexible displays.

Wang and co-workers [141] used carbonized silk nanofibers (CSilkNMs) to fabricate skin-like pressure sensors. Ultra-thin CSilkNMs were obtained from the silk of the silkworm Bombyx mori by electrospinning and carbonization at 800°C. The sensors were constructed from CSilkNMs and microstructured polydimethylsiloxane (PDMS) films which a flexible substrate exhibited excellent properties, including high sensitivity (34.47 kPa^{-1}) over a wide pressure range, ultra-low detection limit (0.8 Pa), the fast response time (<16.7 ms) and high durability (>10,000 cycles). The superb performance makes it suitable for successful application monitoring human physiological signals.

Xiong and co-workers [142] presented the first example of artificial enzymes derived from silk fibroin. Silk fibroin (SF) extracted from silkworm cocoon silk fibers was converted by one-step carbonization in the temperature range of 500-1000°C under an argon atmosphere into active carbonized nitrogen-rich SFs (CSFs). CSFs have been shown to be highly efficient peroxidase and oxidase mimetics, and their enzymatic activity is highly dependent on the carbonization temperature (higher activity after treatment at higher temperatures). This phenomenon is mainly attributed to the increase in the degree of graphitization and the formation of turbostatic carbon. In addition, the catalytic performance of CSFs can be controlled by near-infrared (NIR) light illumination, which enables the design of an intelligent artificial enzyme system. Such silk derivatives can be employed in photothermal-catalytic cancer therapy and sensing device [142].

In their research, Qi and co-workers [143] described a one-step scalable carbonization process at different temperatures (800, 1000, 1250°C) of two kinds of animal silk, *Antheraea pernyi* silk, and *Bombyx mori* silk. The obtained carbon silk materials retained their original morphology were conductive and mechanically robust. The carbonized silks were successfully used in fluidic fiber generators and solar steam generations.

Shastri and co-workers [144] proposed the synthesis of a new nanocomposite and used it as a cathode material for Li-sulfur batteries. First, sulfur nanosheets (S) were synthesized using a microwave method, which were then anchored on porous carbon materials obtained by carbonization at 900°C of silk cocoon (sC). The S-sC nanocomposite as cathode material exhibited an initial specific capacitance of 1231 mAh/g at 0.05 C, and after 50 cycles, the sample retained a capacity of 997 mAh/g.

Jia and co-workers [145] constructed a 3D water evaporator based on a carbonized silkworm cocoon. After carbonization at different temperatures (250-300°C), the carbon material was equipped with super-absorbent polymers (SAPs) and applied to a solar-powered water evaporator device. The evaporator made of the carbonized material at 275°C was durable, exhibited better optical absorption than other water evaporators, and had more efficient water transport, promoting rapid steam generation. The study highlights the potential application of such a solar-powered evaporator for efficient water evaporation and wastewater treatment.

In 2020, Wang and co-workers [146] obtained carbon dots (MSC-CDs) from mulberry silkworm cocoons (MSC) carbonization by high-temperature modified pyrolysis. The carbon materials obtained had a diameter of 2.26-9.35 nm and exhibited good solubility and bioactivity. Pharmacodynamic studies in three animal models confirmed the anti-inflammatory activity, which could be related to the inhibition of interleukin-6 (IL-6) and tumor necrosis factor-α expression (TNF). MSC-CDs provide material for further research in biomedicine and medicine.

Recently, for the first time, silk was used as a carbon precursor to produce a carbon fiber/ceramic composite. Li and co-workers [147] presented a one-step method in which

ceramization of ceramic precursors and carbonization of silk fabric/silk cocoon occurred simultaneously. The resulting composite exhibited excellent electrothermal performance and is a promising material for an electrothermal conversion application.

4. Future Perspective

The use of renewable biological materials such as cellulose, chitin, keratin, spongin, and silk to synthesize carbons is a revolutionary trend in materials science. These approaches affect the reduction of biomass waste, which positively impacts the environment. Additionally, the obtained carbon materials are biodegradable, biocompatible, non-toxic, and precursors are derived from renewable resources. Although research on their preparation has been going on for several years, there is still a need to improve the synthesis and optimization of carbonization conditions (temperature, pressure, time) because the nature and origin of biological materials are diverse. Also, surface modification and the creation of novel nanocomposites may contribute to the improvement of their properties, which will open the way to countless applications in biotechnology, electronics, biomedicine, etc., including commercial purposes on a large scale.

4. Conclusions

Biological materials science is a rewarding area of research in the field of materials science, bringing evolutionary insights into living organisms and inspiration for biomimetic research. The growing environmental awareness of people is causing scientists to pay great attention to research based on biological materials that are easily modifiable yet ecological, renewable, and non-toxic. A lot of interest is directed towards the carbonization process, by which nanoorganized biological materials are transformed into new nanostructured carbon materials with unique properties and positive environmental impact. The possibility of optimization of the process conditions as well as subsequent activation or modification of carbonized materials makes it possible to obtain novel composites at the nanoscale for applications in many technological and environmental fields.

Funding

This research was funded by the National Science Centre within the framework of the project Maestro No. 2020/38/A/ST5/00151

Acknowledgments

This research has no acknowledgment.

Conflicts of Interest

The authors declare no conflict of interest.

References

1. Schobert, H. Carbonization and coking of coal. In *Chemistry of Fossil Fuels and Biofuels*; Cambridge University Press, **2013**; pp. 415–434, https://doi.org/10.1017/CBO9780511844188.
2. Krylova, A.Y.; Zaitchenko, V.M. Hydrothermal Carbonization of Biomass: A Review. *Solid Fuel Chem.* **2018**, *52*, 91–103, https://doi.org/10.3103/S0361521918020076.

3. Corriveau, R.A.; Huh, G.S.; Shatz, C.J. Regulation of class I MHC gene expression in the developing and mature CNS by neural activity. *Neuron* **1998**, *21*, 505–520, https://doi.org/10.1016/S0896-6273(00)80562-0.
4. Ehrlich, H. Biological Materials of Marine Origin : Vertebrates, Springer, **2015**, http://dx.doi.org/10.1007/978-94-007-5730-1..
5. Ehrlich, H. Marine biological materials of Invertebrate origin, Springer, **2019,** http://dx.doi.org/10.1007/978-3-319-92483-0.
6. Meyers, M.; Chen, P.; Lin, A.; Science, Y.S.-P. in materials; 2008, U. Biological materials: structure and mechanical properties. *Elsevier* **2008**, https://doi.org/10.1016/j.pmatsci.2007.05.002.
7. Ehrlich, H. Extreme biomimetics, Springer, **2017**, https://doi.org/10.1007/978-3-319-45340-8.
8. Khrunyk, Y.; Lach, S.; Petrenko, I.; Ehrlich, H. Progress in Modern Marine Biomaterials Research. *Mar. Drugs* **2020**, *18*, https://doi.org/10.3390/md18120589.
9. Lazarus, B.S.; Velasco-Hogan, A.; Gómez-del Río, T.; Meyers, M.A.; Jasiuk, I. A review of impact resistant biological and bioinspired materials and structures. *J. Mater. Res. Technol.* **2020**, *9*, 15705–15738, https://doi.org/10.1016/j.jmrt.2020.10.062.
10. Szatkowski, T.; Siwínska-Stefánska, K.; Wysokowski, M.; Stelling, A.L.; Joseph, Y.; Ehrlich, H.; Jesionowski, T. Immobilization of titanium(IV) oxide onto 3D spongin scaffolds of marine sponge origin according to extreme biomimetics principles for removal of C.I. basic blue 9. *Biomimetics* **2017**, *2*, https://doi.org/10.3390/biomimetics2020004.
11. Petrenko, I.; Summers, A.P.; Simon, P.; Zółtowska-Aksamitowska, S.; Motylenko, M.; Schimpf, C.; Rafaja, D.; Roth, F.; Kummer, K.; Brendler, E.; *et al.* Extreme biomimetics: Preservation of molecular detail in centimeter-scale samples of biological meshes laid down by sponges. *Sci. Adv.* **2019**, *5*, 1–12, https://doi.org/10.1126/sciadv.aax2805.
12. Cho, S.Y.; Yun, Y.S.; Lee, S.; Jang, D.; Park, K.Y.; Kim, J.K.; Kim, B.H.; Kang, K.; Kaplan, D.L.; Jin, H.J. Carbonization of a stable β-sheet-rich silk protein into a pseudographitic pyroprotein. *Nat. Commun.* **2015**, *6*, http://dx.doi.org/10.1038/ncomms8145.
13. Wang, Q.; Yanzhang, R.; Wu, Y.; Zhu, H.; Zhang, J.; Du, M.; Zhang, M.; Wang, L.; Zhang, X.; Liang, X. Silk-derived graphene-like carbon with high electrocatalytic activity for oxygen reduction reaction. *RSC Adv.* **2016**, https://doi.org/10.1039/C6RA07075B.
14. Cho, H.E.; Seo, S.J.; Khil, M.S.; Kim, H. Preparation of carbon nanoweb from cellulose nanowhisker. *Fibers Polym.* **2015**, *16*, 271–275, https://doi.org/10.1007/s12221-015-0271-y.
15. Deng, L.; Young, R.J.; Kinloch, I.A.; Abdelkader, A.M.; Holmes, S.M.; De Haro-Del Rio, D.A.; Eichhorn, S.J. Supercapacitance from cellulose and carbon nanotube nanocomposite fibers. *ACS Appl. Mater. Interfaces* **2013**, *5*, 9983–9990, https://doi.org/10.1021/am403622v.
16. Gao, Y.; Chen, X.; Zhang, J.; Yan, N. Chitin-Derived Mesoporous, Nitrogen-Containing Carbon for Heavy-Metal Removal and Styrene Epoxidation. *Chempluschem* **2015**, *80*, 1556–1564, https://doi.org/10.1002/cplu.201500293.
17. Nguyen, T.D.; Shopsowitz, K.E.; MacLachlan, M.J. Mesoporous nitrogen-doped carbon from nanocrystalline chitin assemblies. *J. Mater. Chem. A* **2014**, *2*, 5915–5921, http://dx.doi.org/10.1039/C3TA15255C.
18. Qian, W.; Sun, F.; Xu, Y.; Qiu, L.; Liu, C.; Wang, S.; Yan, F. Human hair-derived carbon flakes for electrochemical supercapacitors. *Energy Environ. Sci.* **2014**, *7*, 379–386, https://doi.org/10.1039/C3EE43111H.
19. Belarmino, D.D.; Ladchumananandasivam, R.; Belarmino, L.D.; Pimentel, J.R. de M.; da Rocha, B.G.; Galvão, A.O.; de Andrade, S.M.B. Physical and Morphological Structure of Chicken Feathers (Keratin Biofiber) in Natural, Chemically and Thermally Modified Forms. *Mater. Sci. Appl.* **2012**, *03*, 887–893, http://dx.doi.org/10.4236/msa.2012.312129.
20. Szatkowski, T.; Kopczyński, K.; Motylenko, M.; Borrmann, H.; Mania, B.; Graś, M.; Lota, G.; Bazhenov, V. V; Rafaja, D.; Roth, F.; *et al.* Extreme biomimetics: A carbonized 3D spongin scaffold as a novel support for nanostructured manganese oxide(IV) and its electrochemical applications. *Nano Res.* **2018**, *11*, 4199–4214, https://doi.org/10.1007/s12274-018-2008-x.
21. Inagaki, M.; Kang, F.; Toyoda, M.; Konno, H. Advanced Materials Science and Engineering of Carbon. *Adv. Mater. Sci. Eng. Carbon* **2013**, 1–434, https://doi.org/10.1016/C2012-0-03601-0.
22. Naik, R.R.; Singamaneni, S. Introduction: Bioinspired and Biomimetic Materials. *Chem. Rev.* **2017**, *117*, 12581–12583, https://doi.org/10.1021/acs.chemrev.7b00552.
23. Shen, Y. A review on hydrothermal carbonization of biomass and plastic wastes to energy products. *Biomass and Bioenergy* **2020**, *134*, http://dx.doi.org/10.1016/j.biombioe.2020.105479.
24. Green, P.; Barra, A.; Nunes, C.; Ruiz-Hitzky, E.; Ferreira, P. Green Carbon Nanostructures for Functional Composite Materials. *Int. J. Mol. Sci.* **2022**, *23*, 1848, http://dx.doi.org/10.3390/ijms23031848.
25. Cao, X.; Zhu, B.; Zhang, X.; Dong, H. Polymyxin B immobilized on cross-linked cellulose microspheres for endotoxin adsorption. *Carbohydr. Polym.* **2016**, *136*, 12–18, http://dx.doi.org/10.1016/j.carbpol.2015.09.012.
26. Perepelkin, K.E. Renewable plant resources and processed products in chemical fibre production. *Fibre*

Chem. **2004**, *36*, 161–176, https://doi.org/10.1023/B:FICH.0000037977.65328.4e.
27. Klemm, D.; Heublein, B.; Fink, H.P.; Bohn, A. Cellulose: Fascinating biopolymer and sustainable raw material. *Angew. Chemie - Int. Ed.* **2005**, *44*, 3358–3393, http://dx.doi.org/10.1002/anie.200460587.
28. Huber, T.; Müssig, J.; Bremen, H.; Curnow, O. A critical review of all-cellulose composites NF-CompPlus View project NETFIB-Valorization of fibres from nettle grown on marginal lands in an agro-forestry cropping system View project. *Artic. J. Mater. Sci.* **2012**, http://dx.doi.org/10.1007/s10853-011-5774-3.
29. Silva, S.S.; Fernandes, E.M.; Pina, S.; Silva-Correia, J.; Vieira, S.; Oliveira, J.M.; Reis, R.L. 2.11 Polymers of Biological Origin. *Compr. Biomater. II* **2017**, 228–252, https://doi.org/10.1016/B978-0-12-803581-8.10134-1.
30. Shao, W.; Wu, J.; Liu, H.; Ye, S.; Jiang, L.; Liu, X. Novel bioactive surface functionalization of bacterial cellulose membrane. *Carbohydr. Polym.* **2017**, *178*, 270–276, https://doi.org/10.1016/j.carbpol.2017.09.045.
31. Nyström, G.; Fall, A.B.; Carlsson, L.; Wågberg, L. Aligned cellulose nanocrystals and directed nanoscale deposition of colloidal spheres. *Cellulose* **2014**, *21*, 1591–1599, http://dx.doi.org/10.1007/s10570-014-0205-7.
32. Brown, A.J. XLIII. - On an acetic ferment which forms cellulose. *J. Chem. Soc. Trans.* **1886**, *49*, 432–439, https://doi.org/10.1039/CT8864900432.
33. Brown, A.J. XIX.—The chemical action of pure cultivations of bacterium aceti. *J. Chem. Soc. Trans.* **1886**, *49*, 172–187, DOI https://doi.org/10.1039/CT8864900172.
34. Zhou, T.; Chen, D.; Jiu, J.; Nge, T.T.; Sugahara, T.; Nagao, S.; Koga, H.; Nogi, M.; Suganuma, K.; Wang, X.; *et al*. Electrically conductive bacterial cellulose composite membranes produced by the incorporation of graphite nanoplatelets in pristine bacterial cellulose membranes. *Express Polym. Lett.* **2013**, *7*, 756–766, http://dx.doi.org/10.3144/expresspolymlett.2013.73.
35. Coburn, M.; Aditya, T.; Allain, J.P.; Jaramillo, C.; Restrepo, A.M. Surface Modification of Bacterial Cellulose for Biomedical Applications. *Int. J. Mol. Sci. 2022, Vol. 23, Page 610* **2022**, *23*, 610, http://dx.doi.org/10.3390/ijms23020610.
36. Zhu, H.; Shen, F.; Luo, W.; Zhu, S.; Zhao, M.; Natarajan, B.; Dai, J.; Zhou, L.; Ji, X.; Yassar, R.S.; *et al.* Low temperature carbonization of cellulose nanocrystals for high performance carbon anode of sodium-ion batteries. *Nano Energy* **2017**, *33*, 37–44, https://doi.org/10.1016/j.nanoen.2017.01.021.
37. Feng, Z.; Odelius, K.; Rajarao, G.K.; Hakkarainen, M. Microwave carbonized cellulose for trace pharmaceutical adsorption. *Chem. Eng. J.* **2018**, *346*, 557–566, https://doi.org/10.1016/j.cej.2018.04.014.
38. Sheng, K.; Zhang, S.; Liu, J.; E, S.; Jin, C.; Xu, Z.; Zhang, X. Hydrothermal carbonization of cellulose and xylan into hydrochars and application on glucose isomerization. *J. Clean. Prod.* **2019**, *237*, https://doi.org/10.1016/j.jclepro.2019.117831.
39. Yu, K.; Wang, J.; Song, K.; Wang, X.; Liang, C.; Dou, Y. Hydrothermal synthesis of cellulose-derived carbon nanospheres from corn straw as anode materials for lithium ion batteries. *Nanomaterials* **2019**, *9*, https://doi.org/10.3390/nano9010093.
40. Karin H. Adolfsson, Chia-feng Lin, and M.H.-I.& E. Oxidized carbonized cellulose-coated filters for environmental contaminant adsorption and detection. *ACS Publ.* **2020**, *59*, 13578–13587, https://doi.org/10.1021/acs.iecr.0c01973.
41. Bengtsson, A.; Hecht, P.; Sommertune, J.; Ek, M.; Sedin, M.; Sjöholm, E. Carbon Fibers from Lignin-Cellulose Precursors: Effect of Carbonization Conditions. *ACS Sustain. Chem. Eng.* **2020**, *8*, 6826–6833, https://doi.org/10.1021/acssuschemeng.0c01734.
42. Meng, Y.; Contescu, C.I.; Liu, P.; Wang, S.; Lee, S.H.; Guo, J.; Young, T.M. Understanding the local structure of disordered carbons from cellulose and lignin. *Wood Sci. Technol.* **2021**, *55*, 587–606, https://link.springer.com/article/10.1007/s00226-021-01286-6.
43. Kaya, M.; Mujtaba, M.; Ehrlich, H.; Salaberria, A.M.; Baran, T.; Amemiya, C.T.; Galli, R.; Akyuz, L.; Sargin, I.; Labidi, J. On chemistry of γ-chitin. *Carbohydr. Polym.* **2017**, *176*, 177–186, https://doi.org/10.1016/j.carbpol.2017.08.076.
44. Liu, C.; Zhang, H.; Xiao, R.; Wu, S. Value-added organonitrogen chemicals evolution from the pyrolysis of chitin and chitosan. *Carbohydr. Polym.* **2017**, *156*, 118–124, https://doi.org/10.1016/j.carbpol.2016.09.024.
45. Tsurkan, M. V.; Voronkina, A.; Khrunyk, Y.; Wysokowski, M.; Petrenko, I.; Ehrlich, H. Progress in chitin analytics. *Carbohydr. Polym.* **2021**, *252*, https://doi.org/10.1016/J.CARBPOL.2020.117204.
46. Qu, J.; Geng, C.; Lv, S.; Shao, G.; Ma, S.; Wu, M. Nitrogen, oxygen and phosphorus decorated porous carbons derived from shrimp shells for supercapacitors. *Electrochim. Acta* **2015**, *176*, 982–988, http://doi.org/10.1016/j.carbpol.2020.117204.
47. Zhou, J.; Bao, L.; Wu, S.; Yang, W.; Wang, H. Chitin based heteroatom-doped porous carbon as electrode materials for supercapacitors. *Carbohydr. Polym.* **2017**, *173*, 321–329, https://doi.org/10.1016/j.carbpol.2017.06.004.
48. Brunner, E.; Richthammer, P.; Ehrlich, H.; Paasch, S.; Simon, P.; Ueberlein, S.; Van Pée, K.H. Chitin-based organic networks: An integral part of cell wall biosilica in the diatom thalassiosira pseudonana. *Angew. Chemie - Int. Ed.* **2009**, *48*, 9724–9727, https://doi.org/10.1002/anie.200905028.
49. Bo, M.; Bavestrello, G.; Kurek, D.; Paasch, S.; Brunner, E.; Born, R.; Galli, R.; Stelling, A.L.; Sivkov, V.N.;

Petrova, O. V.; *et al*. Isolation and identification of chitin in the black coral Parantipathes larix (Anthozoa: Cnidaria). *Int. J. Biol. Macromol.* **2012**, *51*, 129–137, https://doi.org/10.1016/j.ijbiomac.2012.04.016.
50. Nowacki, K.; Stępniak, I.; Langer, E.; Tsurkan, M.; Wysokowski, M.; Petrenko, I.; Khrunyk, Y.; Fursov, A.; Bo, M.; Bavestrello, G.; *et al*. Electrochemical approach for isolation of chitin from the skeleton of the black coral cirrhipathes sp. (Antipatharia). *Mar. Drugs* **2020**, *18*, https://doi.org/10.3390/md18060297.
51. Ehrlich, H.; Shaala, L.A.; Youssef, D.T.A.; Zoltowska-Aksamitowska, S.; Tsurkan, M.; Galli, R.; Meissner, H.; Wysokowski, M.; Petrenko, I.; Tabachnick, K.R.; *et al*. Discovery of chitin in skeletons of non-verongiid Red Sea demosponges. *PLoS One* **2018**, *13*, https://doi.org/10.1371/journal.pone.0195803.
52. Kovalchuk, V.; Voronkina, A.; Binnewerg, B.; Schubert, M.; Muzychka, L.; Wysokowski, M.; Tsurkan, M. V; Bechmann, N.; Petrenko, I.; Fursov, A.; *et al*. Naturally drug-loaded chitin: Isolation and applications. *Mar. Drugs* **2019**, *17*, 574, https://doi.org/10.3390/md17100574.
53. Schubert, M.; Binnewerg, B.; Voronkina, A.; Muzychka, L.; Wysokowski, M.; Petrenko, I.; Kovalchuk, V.; Tsurkan, M.; Martinovic, R.; Bechmann, N.; *et al*. Naturally prefabricated marine biomaterials: Isolation and applications of flat chitinous 3D scaffolds from Ianthella labyrinthus (demospongiae: Verongiida). *Int. J. Mol. Sci.* **2019**, *20*, 5105, https://doi.org/10.3390/ijms20205105.
54. Nowacki, K.; Stępniak, I.; Machałowski, T.; Wysokowski, M.; Petrenko, I.; Schimpf, C.; Rafaja, D.; Langer, E.; Richter, A.; Ziętek, J.; *et al*. Electrochemical method for isolation of chitinous 3D scaffolds from cultivated Aplysina aerophoba marine demosponge and its biomimetic application. *Appl. Phys. A Mater. Sci. Process.* **2020**, *126*, https://doi.org/10.1007/s00339-020-03533-2.
55. Talevski, T.; Talevska Leshoska, A.; Pejoski, E.; Pejin, B.; Machałowski, T.; Wysokowski, M.; Tsurkan, M. V.; Petrova, O.; Sivkov, V.; Martinovic, R.; *et al*. Identification and first insights into the structure of chitin from the endemic freshwater demosponge Ochridaspongia rotunda (Arndt, 1937). *Int. J. Biol. Macromol.* **2020**, *162*, 1187–1194, https://doi.org/10.1016/j.ijbiomac.2020.06.247.
56. Machałowski, T.; Wysokowski, M.; Tsurkan, M. V.; Galli, R.; Schimpf, C.; Rafaja, D.; Brendler, E.; Viehweger, C.; Żółtowska-Aksamitowska, S.; Petrenko, I.; *et al*. Spider chitin: An Ultrafast Microwave-Assisted Method for Chitin Isolation from Caribena versicolor Spider Molt Cuticle. *Molecules* **2019**, *24*, https://doi.org/10.3390/molecules24203736.
57. Machałowski, T.; Wysokowski, M.; Żółtowska-Aksamitowska, S.; Bechmann, N.; Binnewerg, B.; Schubert, M.; Guan, K.; Bornstein, S.R.; Czaczyk, K.; Pokrovsky, O.; *et al*. Spider Chitin. The biomimetic potential and applications of Caribena versicolor tubular chitin. *Carbohydr. Polym.* **2019**, *226*, https://doi.org/10.1016/j.carbpol.2019.115301.
58. Rinaudo, M. Chitin and chitosan: Properties and applications. *Prog. Polym. Sci.* **2006**, *31*, 603–632, https://doi.org/10.1016/j.progpolymsci.2006.06.001.
59. Ehrlich, H. Chitin and collagen as universal and alternative templates in biomineralization. *Int. Geol. Rev.* **2010**, *52*, 661–699, https://doi.org/10.1080/00206811003679521.
60. Kertmen, A.; Petrenko, I.; Schimpf, C.; Rafaja, D.; Petrova, O.; Sivkov, V.; Nekipelov, S.; Fursov, A.; Stelling, A.L.; Heimler, K.; *et al*. Calcite Nanotuned Chitinous Skeletons of Giant Ianthella basta Marine Demosponge. *mdpi.com* **2021**, https://doi.org/10.3390/ijms222212588.
61. Nikolov, S.; Fabritius, H.; Petrov, M.; Friák, M.; Lymperakis, L.; Sachs, C.; Raabe, D.; Neugebauer, J. Robustness and optimal use of design principles of arthropod exoskeletons studied by ab initio-based multiscale simulations. *J. Mech. Behav. Biomed. Mater.* **2011**, *4*, 129–145, https://doi.org/10.1016/j.jmbbm.2010.09.015.
62. Ehrlich, H. Chitin of Poriferan Origin as a Unique Biological Material. *Blue Biotechnol.* **2018**, 821–854, https://doi.org/10.1002/9783527801718.ch26.
63. Mutsenko, V.; Gryshkov, O.; Rogulska, O.; Lode, A.; Petrenko, A.Y.; Gelinsky, M.; Glasmacher, B.; Ehrlich, H. Chitinous scaffolds from marine sponges for tissue engineering. *Springer Ser. Biomater. Sci. Eng.* **2019**, *14*, 285–307, http://dx.doi.org/10.1007/978-981-13-8855-2_13.
64. Binnewerg, B.; Schubert, M.; Voronkina, A.; Muzychka, L.; Wysokowski, M.; Petrenko, I.; Djurović, M.; Kovalchuk, V.; Tsurkan, M.; Martinovic, R.; *et al*. Marine biomaterials: Biomimetic and pharmacological potential of cultivated Aplysina aerophoba marine demosponge. *Mater. Sci. Eng. C* **2020**, *109*, https://doi.org/10.1016/j.msec.2019.110566.
65. Wysokowski, M.; Petrenko, I.; Stelling, A.L.; Stawski, D.; Jesionowski, T.; Ehrlich, H. Poriferan chitin as a versatile template for extreme biomimetics. *Polymers (Basel).* **2015**, *7*, 235–265, https://doi.org/10.3390/polym7020235.
66. Klinger, C.; Ółtowska-Aksamitowska, S.Z.; Wysokowski, M.; Tsurkan, M. V; Galli, R.; Petrenko, I.; Machałowski, T.; Ereskovsky, A.; Martinović, R.; Muzychka, L.; *et al*. Express method for isolation of ready-to-use 3D chitin scaffolds from aplysina archeri (aplysineidae: verongiida) demosponge. *Mar. Drugs* **2019**, *17*, 131, https://doi.org/10.3390/md17020131.
67. Tsurkan, D.; Wysokowski, M.; Petrenko, I.; Voronkina, A.; Khrunyk, Y.; Fursov, A.; Ehrlich, H. Modern scaffolding strategies based on naturally pre-fabricated 3D biomaterials of poriferan origin. *Appl. Phys. A Mater. Sci. Process.* **2020**, *126*, https://doi.org/10.1007/s00339-020-03564-9.
68. Kertmen, A.; Ehrlich, H. Patentology of chitinous biomaterials. Part I: Chitin. *Carbohydr. Polym.* **2022**, *282*, https://doi.org/10.1016/j.carbpol.2022.119102.

69. Duan, B.; Gao, X.; Yao, X.; Fang, Y.; Huang, L.; Zhou, J.; Zhang, L. Unique elastic N-doped carbon nanofibrous microspheres with hierarchical porosity derived from renewable chitin for high rate supercapacitors. *Nano Energy* **2016**, *27*, 482–491, https://doi.org/10.1016/j.nanoen.2016.07.034.
70. Wang, Y.; Liu, R.; Tian, Y.; Sun, Z.; Huang, Z.; Wu, X.; Li, B. Heteroatoms-doped hierarchical porous carbon derived from chitin for flexible all-solid-state symmetric supercapacitors. *Chem. Eng. J.* **2020**, *384*, https://doi.org/10.1016/j.cej.2019.123263.
71. Zheng, S.; Cui, Y.; Zhang, J.; Gu, Y.; Shi, X.; Peng, C.; Wang, D. Nitrogen doped microporous carbon nanospheres derived from chitin nanogels as attractive materials for supercapacitors. *RSC Adv.* **2019**, *9*, 10976–10982, https://doi.org/10.1039/C9RA00683D.
72. Jiang, Q.; Jing, Y.; Wang, J.; Ni, Y.; Gao, R.; Wang, Y.; Zhang, J.; Yin, H. Lignosulfonate for improving electrochemical performance of chitin derived carbon materials as a superior anode for lithium-ion batteries. *J. Alloys Compd.* **2021**, *885*, https://doi.org/10.1016/J.JALLCOM.2021.160973.
73. Goodrich, J.D.; Winter, W.T. α-Chitin Nanocrystals Prepared from Shrimp Shells and Their Specific Surface Area Measurement. *Biomacromolecules* **2006**, *8*, 252–257, https://doi.org/10.1021/bm0603589.
74. Wu, P.; Li, W.; Wu, Q.; Liu, Y.; Liu, S. Hydrothermal synthesis of nitrogen-doped carbon quantum dots from microcrystalline cellulose for the detection of Fe3+ ions in an acidic environment. *RSC Adv.* **2017**, *7*, 44144–44153, https://doi.org/10.1039/C7RA08400E.
75. Gedda, G.; Lee, C.Y.; Lin, Y.C.; Wu, H.F. Green synthesis of carbon dots from prawn shells for highly selective and sensitive detection of copper ions. *Sensors Actuators B Chem.* **2016**, *224*, 396–403, https://doi.org/10.1016/j.snb.2015.09.065.
76. Naghdi, T.; Atashi, M.; Golmohammadi, H.; Pourreza, N.; Saeedi, I.; Alanezhad, M. Title: Carbon quantum dots originated from chitin nanofibers as a fluorescent chemoprobe for drug sensing. **2017**, https://doi.org/10.1016/j.jiec.2017.03.039.
77. Jiang, Q.; Jing, Y.; Ni, Y.; Gao, R.; Zhou, P. Potentiality of carbon quantum dots derived from chitin as a fluorescent sensor for detection of ClO−. *Microchem. J.* **2020**, *157*, https://doi.org/10.1016/j.microc.2020.105111.
78. Ji, Q.; Li, H. High surface area activated carbon derived from chitin for efficient adsorption of Crystal Violet. *Diam. Relat. Mater.* **2021**, *118*, http://doi.org/10.1016/j.diamond.2021.108516.
79. Khanday, W.A.; Ahmed, M.J.; Okoye, P.U.; Hummadi, E.H.; Hameed, B.H. Single-step pyrolysis of phosphoric acid-activated chitin for efficient adsorption of cephalexin antibiotic. *Bioresour. Technol.* **2019**, *280*, 255–259, https://doi.org/10.1016/j.biortech.2019.02.003.
80. McLellan, J.; Thornhill, S.G.; Shelton, S.; Kumar, M. Keratin-Based Biofilms, Hydrogels, and Biofibers. In; **2019**; pp. 187–200, http://dx.doi.org/10.1007/978-3-030-02901-2_7.
81. Fudge, D.S.; Winegard, T.; Ewoldt, R.H.; Beriault, D.; Szewciw, L.; McKinley, G.H. From ultra-soft slime to hard α-keratins: The many lives of intermediate filaments. *Integr. Comp. Biol.* **2009**, *49*, 32–39, https://doi.org/10.1093/icb/icp007.
82. Hearle, J.W.S. A critical review of the structural mechanics of wool and hair fibres. *Int. J. Biol. Macromol.* **2000**, *27*, 123–138, https://doi.org/10.1016/s0141-8130(00)00116-1.
83. Schweizer, J.; Bowden, P.E.; Coulombe, P.A.; Langbein, L.; Lane, E.B.; Magin, T.M.; Maltais, L.; Omary, M.B.; Parry, D.A.D.; Rogers, M.A.; *et al.* New consensus nomenclature for mammalian keratins. *J. Cell Biol.* **2006**, *174*, 169–174, https://doi.org/10.1083/jcb.200603161.
84. Mi, X.; Chang, Y.; Xu, H.; Yang, Y. Valorization of keratin from food wastes via crosslinking using non-toxic oligosaccharide derivatives. *Food Chem.* **2019**, *300*, https://doi.org/10.1016/j.foodchem.2019.125181.
85. Shavandi, A.; Silva, T.; Bekhit, A.; Science, A.B.-B.; 2017, U. Keratin: dissolution, extraction and biomedical application. *pubs.rsc.org* **2017**, *5*, 1699, https://doi.org/10.1039/C7BM00411G.
86. Idrees, H.; Zaidi, S.Z.J.; Sabir, A.; Khan, R.U.; Zhang, X.; Hassan, S.U. A review of biodegradable natural polymer-based nanoparticles for drug delivery applications. *Nanomaterials* **2020**, *10*, 1–22.
87. Feroz, S.; Muhammad, N.; Ranayake, J.; Dias, G. Keratin - Based materials for biomedical applications. *Bioact. Mater.* **2020**, *5*, 496–509, https://doi.org/10.1016/j.bioactmat.2020.04.007.
88. Chilakamarry, C.R.; Mahmood, S.; Saffe, S.N.B.M.; Arifin, M.A. Bin; Gupta, A.; Sikkandar, M.Y.; Begum, S.S.; Narasaiah, B. Extraction and application of keratin from natural resources: a review. *3 Biotech* **2021**, *11*, 220, https://doi.org/10.1007/s13205-021-02734-7.
89. Chaudhari, K.N.; Song, M.Y.; Yu, J.-S. Transforming Hair into Heteroatom-Doped Carbon with High Surface Area. **2014**, https://doi.org/10.1002/smll.201303831.
90. Kreplak, L.; Franbourg, A.; Briki, F.; Leroy, F.; Dallé, D.; Doucet, J. A new deformation model of hard α-keratin fibers at the nanometer scale: Implications for hard α-keratin intermediate filament mechanical properties. *Biophys. J.* **2002**, *82*, 2265–2274, https://doi.org/10.1016/s0006-3495(02)75572-0.
91. Pramanick, B.; Cadenas, L.B.; Kim, D.M.; Lee, W.; Shim, Y.B.; Martinez-Chapa, S.O.; Madou, M.J.; Hwang, H. Human hair-derived hollow carbon microfibers for electrochemical sensing. *Carbon N. Y.* **2016**, *107*, 872–877, https://doi.org/10.1016/j.carbon.2016.06.095.
92. Ahmed, M.; Azhrul Islam, M.; Asif, M.; Hameed, B. Human hair-derived high surface area porous carbon material for the adsorption isotherm and kinetics of tetracycline antibiotics. *Bioresour. Technol.* **2017**, https://doi.org/10.1016/j.biortech.2017.06.174.

93. Zhao, Z.Q.; Xiao, P.W.; Zhao, L.; Liu, Y.; Han, B.H. Human hair-derived nitrogen and sulfur co-doped porous carbon materials for gas adsorption. *RSC Adv.* **2015**, *5*, 73980–73988, https://doi.org/10.1039/C5RA15690D.
94. Freitas, F.S.; Gonçalves, A.S.; De Morais, A.; Benedetti, J.E.; Nogueira, A.F. Graphene-like MoS2 as a low-cost counter electrode material for dye-sensitized solar cells. *NanoGe J. Energy Sustain.* **2012**, 11002–11003.
95. Sahasrabudhe, A.; Kapri, S.; Bhattacharyya, S. Graphitic porous carbon derived from human hair as 'green' counter electrode in quantum dot sensitized solar cells. *Carbon N. Y.* **2016**, *107*, 395–404, http://dx.doi.org/10.1016%2Fj.carbon.2016.06.015.
96. Si, W.; Zhou, J.; Zhang, S.; Li, S.; Xing, W.; Zhuo, S. Tunable N-doped or dual N, S-doped activated hydrothermal carbons derived from human hair and glucose for supercapacitor applications. *Electrochim. Acta* **2013**, *107*, 397–405, https://doi.org/10.1016/j.electacta.2013.06.065.
97. Satish, R.; Vanchiappan, A.; Wong, C.L.; Ng, K.W.; Srinivasan, M. Macroporous carbon from human hair: A journey towards the fabrication of high energy Li-ion capacitors. *Electrochim. Acta* **2015**, *182*, 474–481, http://dx.doi.org/10.1016/j.electacta.2015.09.127.
98. Sinha, P.; Yadav, A.; Tyagi, A.; Paik, P.; Yokoi, H.; Naskar, A.K.; Kuila, T.; Kar, K.K. Keratin-derived functional carbon with superior charge storage and transport for high-performance supercapacitors. *Carbon N. Y.* **2020**, *168*, 419–438, https://doi.org/10.1016/j.carbon.2020.07.007.
99. Martin Parrondo, R.; Bagriantsev, D. Personalised synthetic diamond of different colours, obtained from (living or dead) human or animal keratin and production method thereof, **2005**.
100. Chatzimitakos, T.G.; Kasouni, A.I.; Troganis, A.N.; Stalikas, C.D. Carbonization of human fingernails: toward the sustainable production of multifunctional nitrogen and sulfur codoped carbon nanodots with highly luminescent. *ACS Publ.* **2018**, *10*, 16024–16032, https://doi.org/10.1021/acsami.8b03263.
101. Senoz, E.; Wool, R.P. Microporous carbon-nitrogen fibers from keratin fibers by pyrolysis. *J. Appl. Polym. Sci.* **2010**, *118*, 1752–1765, https://doi.org/10.1002/app.32397.
102. Wang, Q.; Cao, Q.; Wang, X.; Jing, B.; Kuang, H.; Zhou, L. A high-capacity carbon prepared from renewable chicken feather biopolymer for supercapacitors. *J. Power Sources* **2013**, *225*, 101–107, https://doi.org/10.1016/j.jpowsour.2012.10.022.
103. Hastuti, E.; Irfana, I. Effect of PVDF composition in activated carbon derived from chicken feather on electrical properties. *Journal of Physics: Conference Series*; **2021**; Vol. 1825, http://dx.doi.org/10.1088/1742-6596/1825/1/012052.
104. Tyagi, A.; Yadav, A.; Sinha, P.; Singh, S.; Paik, P.; Kar, K.K. Chicken feather rachis: An improvement over feather fiber derived electrocatalyst for oxygen electroreduction. *Appl. Surf. Sci.* **2019**, *495*, https://doi.org/10.1016/j.apsusc.2019.143603.
105. Zulaiha, S.; Adawiyah, N.; Soleman Ritonga, P.; Sultan Syarif Kasim Riau, N.; Hilir, I. Chicken Feather Activated Carbon as an Adsorbent and It's Application in Chemistry Learning. *Int. J. Res. Publ. Rev.* **2021**.
106. Chen, H.; Li, W.; Wang, J.; Xu, H.; Liu, Y.; Zhang, Z.; Li, Y.; Zhang, Y. Adsorption of cadmium and lead ions by phosphoric acid-modified biochar generated from chicken feather: Selective adsorption and influence of dissolved organic matter. *Bioresour. Technol.* **2019**, *292*, 121948, https://doi.org/10.1016/j.biortech.2019.121948.
107. Paul, E.; Nwokem, N.; Anumonye, F.U. Biosorption of Nickel (II) from aqueous solution onto activated carbon prepared from chicken feather. *J. Appl. Sci. Environ. Manag.* **2019**, *23*, 1057, https://doi.org/10.4314/jasem.v23i6.9.
108. Rahmani-Sani, A.; Singh, P.; Raizada, P.; Claudio Lima, E.; Anastopoulos, I.; Giannakoudakis, D.A.; Sivamani, S.; Dontsova, T.A.; Hosseini-Bandegharaei, A. Use of chicken feather and eggshell to synthesize a novel magnetized activated carbon for sorption of heavy metal ions. *Bioresour. Technol.* **2020**, *297*, https://doi.org/10.1016/j.biortech.2019.122452.
109. Hastuti, E.; Subhan, A.; Auwala, A. Performance of carbon based on chicken feather with KOH activation as an anode for Li-ion batteries. *Materials Today: Proceedings*; **2020**; Vol. 44, pp. 3183–3187, http://dx.doi.org/10.1016/j.matpr.2020.11.429.
110. Muthukumaraswamy Rangaraj, V.; Achazhiyath Edathil, A.; Kadirvelayutham, P.; Banat, F. Chicken feathers as an intrinsic source to develop ZnS/carbon composite for Li-ion battery anode material. *Mater. Chem. Phys.* **2020**, *248*, https://doi.org/10.1016/j.matchemphys.2020.122953.
111. Villanueva, J.L.; Tapas, G.A.; Bayot, J.S.; Marquez, M.C.; Aquino, R.R. Electrospun Polyacrylonitrile-Keratin Derived Carbon Nanofiber as Electrode for Asymmetric Supercapacitor. *Key Eng. Mater.* **2021**, *878*, 56–61, https://doi.org/10.4028/www.scientific.net/KEM.878.56.
112. Tsurkan, D.; Simon, P.; Schimpf, C.; Motylenko, M.; Rafaja, D.; Roth, F.; Inosov, D.S.; Makarova, A.A.; Stepniak, I.; Petrenko, I.; *et al.* Extreme Biomimetics: Designing of the First Nanostructured 3D Spongin–Atacamite Composite and its Application. *Wiley Online Libr.* **2021**, *33*, https://doi.org/10.1002/adma.202101682.
113. Pronzato, R.; Bavestrello, G.; Cerrano, C.; Magnino, G.; Manconi, R.; Pantelis, J.; Sarà, A.; Sidri, M. Sponge farming in the Mediterranean Sea: New perspectives. *Mem. Queensl. Museum* **1999**, *44*, 485–491.
114. Ehrlich, H.; Wysokowski, M.; Zółtowska-Aksamitowska, S.; Petrenko, I.; Jesionowski, T. Collagens of

poriferan origin. *Mar. Drugs* **2018**, *16*, https://doi.org/10.3390/md16030079.
115. Louden, D.; Inderbitzin, S.; Peng, Z.; de Nys, R. Development of a new protocol for testing bath sponge quality. *Aquaculture* **2007**, *271*, 275–285, http://dx.doi.org/10.1016%2Fj.aquaculture.2007.06.010.
116. Jesionowski, T.; Norman, M.; Zółtowska-Aksamitowska, S.; Petrenko, I.; Joseph, Y.; Ehrlich, H. Marine spongin: Naturally prefabricated 3D scaffold-based biomaterial. *Mar. Drugs* **2018**, *16*, https://doi.org/10.3390/md16030088.
117. Szatkowski, T.; Jesionowski, T. Hydrothermal Synthesis of Spongin-Based Materials. *Extrem. Biomimetics* **2016**, 251–274, http://dx.doi.org/10.1007/978-3-319-45340-8_10.
118. Antecka, K.; Zdarta, J.; Zgola-Grzeskowiak, A.; Ehrlich, H.; Jesionowski, T. Degradation of bisphenols using immobilized laccase supported onto biopolymer marine sponge scaffolds: Effect of operational parameters on removal efficiency. *N. Biotechnol.* **2018**, *44*, S163, http://dx.doi.org/10.1016/j.nbt.2018.05.1180.
119. Żółtowska, S.; Koltsov, I.; Alejski, K.; Ehrlich, H.; Ciałkowski, M.; Jesionowski, T. Thermal decomposition behaviour and numerical fitting for the pyrolysis kinetics of 3D spongin-based scaffolds. The classic approach. *Polym. Test.* **2021**, *97*, https://doi.org/10.1016/j.polymertesting.2021.107148.
120. Akbari, M.; Jafari, H.; Rostami, M.; Mahdavinia, G.R.; Nasab, A.S.; Tsurkan, D.; Petrenko, I.; Ganjali, M.R.; Rahimi-Nasrabadi, M.; Ehrlich, H. Adsorption of cationic dyes on a magnetic 3d spongin scaffold with nano-sized Fe3O4 cores. *Mar. Drugs* **2021**, *19*, 512, https://doi.org/10.3390/md19090512.
121. Pozzolini, M.; Tassara, E.; Dodero, A.; Castellano, M.; Vicini, S.; Ferrando, S.; Aicardi, S.; Cavallo, D.; Bertolino, M.; Petrenko, I.; *et al*. Potential biomedical applications of collagen filaments derived from the marine demosponges ircinia oros (Schmidt, 1864) and sarcotragus foetidus (schmidt, 1862). *Mar. Drugs* **2021**, *19*, https://doi.org/10.3390/md19100563.
122. Szatkowski, T.; Wysokowski, M.; Lota, G.; Pęziak, D.; Bazhenov, V. V; Nowaczyk, G.; Walter, J.; Molodtsov, S.L.; Stöcker, H.; Himcinschi, C.; *et al*. Novel nanostructured hematite-spongin composite developed using an extreme biomimetic approach. *RSC Adv.* **2015**, *5*, 79031–79040, https://doi.org/10.1039/C5RA09379A.
123. Szatkowski, T.; Siwínska-Stefánska, K.; Wysokowski, M.; Stelling, A.L.; Joseph, Y.; Ehrlich, H.; Jesionowski, T. Immobilization of titanium(IV) oxide onto 3D spongin scaffolds of marine sponge origin according to extreme biomimetics principles for removal of C.I. basic blue 9. *Biomimetics* **2017**, *2*, https://doi.org/10.3390/biomimetics2020004.
124. Zóltowska, S.; Miñambres, J.F.; Piasecki, A.; Mertens, F.; Jesionowski, T. Three-dimensional commercial-sponge-derived Co3O4@C catalysts for effective treatments of organic contaminants. *J. Environ. Chem. Eng.* **2021**, *9*, https://doi.org/10.1016/j.jece.2021.105631.
125. Żółtowska, S.; Bielan, Z.; Zembrzuska, J.; Siwińska-Ciesielczyk, K.; Piasecki, A.; Zielińska-Jurek, A.; Jesionowski, T. Modification of structured bio-carbon derived from spongin-based scaffolds with nickel compounds to produce a functional catalyst for reduction and oxidation reactions: Potential for use in environmental protection. *Sci. Total Environ.* **2021**, *794*, https://doi.org/10.1016/j.scitotenv.2021.148692.
126. Costa, F.; Silva, R.; Boccaccini, A.R. Fibrous protein-based biomaterials (silk, keratin, elastin, and resilin proteins) for tissue regeneration and repair. In *Peptides and Proteins as Biomaterials for Tissue Regeneration and Repair*; Elsevier, 2018; pp. 175–204, https://doi.org/10.1016/B978-0-08-100803-4.00007-3.
127. Kronenberger, K.; Dicko, C.; Vollrath, F. A novel marine silk. *Naturwissenschaften* **2012**, *99*, 3–10, https://doi.org/10.1007/s00114-011-0853-5.
128. Winkler, S.; Kaplan, D.L. Molecular biology of spider silk. *Rev. Mol. Biotechnol.* **2000**, *74*, 85–93, https://doi.org/10.1016/s1389-0352(00)00005-2.
129. Tokareva, O.; Jacobsen, M.; Buehler, M.; Wong, J.; Kaplan, D.L. Structure-function-property-design interplay in biopolymers: Spider silk. *Acta Biomater.* **2014**, *10*, 1612–1626, https://doi.org/10.1016/j.actbio.2013.08.020.
130. Aigner, T.B.; DeSimone, E.; Scheibel, T. Biomedical Applications of Recombinant Silk-Based Materials. *Adv. Mater.* **2018**, *30*, https://doi.org/10.1002/adma.201704636.
131. Liu, Y.; Shao, Z.; Vollrath, F. Relationships between supercontraction and mechanical properties of spider silk. *Nat. Mater.* **2005**, *4*, 901–905, https://doi.org/10.1038/nmat1534.
132. Omenetto, F.G.; Kaplan, D.L. New opportunities for an ancient material. *Science* **2010**, *329*, 528–531, https://doi.org/10.1126/science.1188936.
133. Eisenberg, D.; Jucker, M. The amyloid state of proteins in human diseases. *Cell* **2012**, *148*, 1188–1203, https://doi.org/10.1016/j.cell.2012.02.022.
134. Strassburg, S.; Zainuddin, S.; Scheibel, T. The Power of Silk Technology for Energy Applications. *Adv. Energy Mater.* **2021**, *11*, https://doi.org/10.1002/aenm.202100519.
135. Wang, C.; Chen, W.; Xia, K.; Xie, N.; Wang, H.; Zhang, Y. Silk-Derived 2D Porous Carbon Nanosheets with Atomically-Dispersed Fe-N x -C Sites for Highly Efficient Oxygen Reaction Catalysts. *Small* **2019**, *15*, https://doi.org/10.1002/smll.201804966.
136. Zhu, B.; Wang, H.; Leow, W.R.; Cai, Y.; Loh, X.J.; Han, M.Y.; Chen, X. Silk Fibroin for Flexible Electronic Devices. *Adv. Mater.* **2016**, *28*, 4250–4265, https://doi.org/10.1002/adma.201504276.

137. Patil, A.B.; Huang, Y.; Ma, L.; Wu, R.; Meng, Z.; Kong, L.; Zhang, Y.; Zhang, W.; Liu, Q.; Liu, X.Y. An efficient disposable and flexible electrochemical sensor based on a novel and stable metal carbon composite derived from cocoon silk. *Biosens. Bioelectron.* **2019**, *142*, https://doi.org/10.1016/j.bios.2019.111595.
138. Taer, E.; Mustika, W.S.; Taslim, R. Synthesis of a Carbon-activated Microfiber from Spider Webs Silk. *In Proceedings of the IOP Conference Series: Earth and Environmental Science; Institute of Physics Publishing*, **2017**; Vol. 58, http://dx.doi.org/10.1088/1755-1315/58/1/012052.
139. Zhou, L.; Fu, P.; Cai, X.; Zhou, S.; Yuan, Y. Naturally derived carbon nanofibers as sustainable electrocatalysts for microbial energy harvesting: A new application of spider silk. *Appl. Catal. B Environ.* **2016**, *188*, 31–38, http://dx.doi.org/10.1016%2Fj.apcatb.2016.01.063.
140. Wang, Y.; Ren, J.; Ye, C.; Pei, Y.; Ling, S. Thermochromic Silks for Temperature Management and Dynamic Textile Displays. *Nano-Micro Lett.* **2021**, *13*, https://doi.org/10.1007/s40820-021-00591-w.
141. Wang, Q.; Jian, M.; Wang, C.; Zhang, Y. Carbonized Silk Nanofiber Membrane for Transparent and Sensitive Electronic Skin. *Adv. Funct. Mater.* **2017**, *27*, https://doi.org/10.1002/adfm.201605657.
142. Xiong, X.; Tang, Y.; Xu, C.; Huang, Y.; Wang, Y.; Fu, L.; Lin, C.; Zhou, D.; Lin, Y. High Carbonization Temperature to Trigger Enzyme Mimicking Activities of Silk-Derived Nanosheets. *Small* **2020**, *16*, https://doi.org/10.1002/smll.202004129.
143. Qi, P.; Ren, J.; Ling, S. Animal Silk-Derived Amorphous Carbon Fibers for Electricity Generation and Solar Steam Evaporation. *Front. Chem.* **2021**, *9*, 239, https://doi.org/10.3389/fchem.2021.669797.
144. Shastri, M.; Sriramoju, J.B.; Muniyappa, M.; Shetty, M.; Gangaraju, V.; Sindhu Sree, M.; Marlingaiah, N.; Kobayashi, H.; Tomai, T.; Honma, I.; *et al*. Silk cocoon derived carbon and sulfur nanosheets as cathode material for Li-S battery application. *Emergent Mater.* **2021**, *4*, 1329–1337, https://doi.org/10.1007/s42247-021-00218-1.
145. Jia, L.; Feng, M.; Zhang, F.; Lin, H.; Guo, W.; Yu, K.; Yang, C.; Qu, F. Three-dimensional water evaporator based on carbonized silkworm cocoon for highly effective solar-driven water evaporation and wastewater purification. *Mater. Lett.* **2022**, *312*, 131661, https://doi.org/10.1016/j.matlet.2022.131661.
146. Wang, X.; Zhang, Y.; Kong, H.; Cheng, J.; Zhang, M.; Sun, Z.; Wang, S.; Liu, J.; Qu, H.; Zhao, Y. Novel mulberry silkworm cocoon-derived carbon dots and their anti-inflammatory properties. *Artif. Cells, Nanomedicine Biotechnol.* **2020**, *48*, 68–76, https://doi.org/10.1080/21691401.2019.1699810.
147. Li, D.; Tang, B.; Lu, X.; Chen, W.; Dong, X.; Wang, J.; Wang, X. Hierarchically carbonized silk/ceramic composites for electrothermal conversion. *Compos. Part A Appl. Sci. Manuf.* **2021**, *141*, 106237, https://doi.org/10.1016/j.compositesa.2020.106237.